Published in final edited form as:
Curr Biol. 2009 December 15; 19(23): 2008–2013. doi:10.1016/j.cub.2009.10.026.

Human Myo19 is a novel myosin that associates with mitochondria

Omar A. Quintero[1,2,3,5], **Melinda M. DiVito**[1], **Rebecca C. Adikes**[3], **Melisa B. Kortan**[2], **Lindsay B. Case**[2], **Audun J. Lier**[2], **Niki S. Panaretos**[2], **Stephanie Q. Slater**[1,3], **Michelle Rengarajan**[4], **Marianela Feliu**[3], and **Richard E. Cheney**[1]

[1]Cell and Molecular Physiology Department, University of North Carolina at Chapel Hill, Chapel Hill, NC 27599, USA

[2]Department of Biology, Franklin and Marshall College, Lancaster, PA, 17603, USA

[3]Department of Biological Sciences, Mount Holyoke College, South Hadley, MA, 01075, USA

[4]Department of Biochemistry, Stanford University, Stanford, CA 94305

[5]Department of Cell and Molecular Physiology, Penn State College of Medicine, Hershey, PA, 17033, USA

Summary

Mitochondria are pleomorphic organelles [1,2] that have central roles in cell physiology. Defects in their localization and dynamics lead to human disease [3-5]. Myosins are actin-based motors that power processes such as muscle contraction, cytokinesis, and organelle transport [6]. Here we report the initial characterization of myosin-XIX (Myo19), the founding member of a novel class of myosin that associates with mitochondria. The 970aa heavy chain consists of a motor domain, three IQ motifs, and a short tail. Myo19 mRNA is expressed in multiple tissues and antibodies to human Myo19 detect a ~109kD band in multiple cell lines. Both endogenous Myo19 and GFP-Myo19 exhibit striking localization to mitochondria. Deletion analysis reveals that the Myo19 tail is necessary and sufficient for mitochondrial localization. Expressing full-length GFP-Myo19 in A549 cells reveals a remarkable gain-of-function where the majority of the mitochondria move continuously. Moving mitochondria travel for many microns with an obvious leading end and distorted shape. The motility and shape-change are sensitive to latrunculin B, indicating that both are actin-dependent. Expressing the GFP-Myo19 tail in CAD cells resulted in decreased mitochondrial run lengths in neurites. These results suggest that this novel myosin functions as an actin-based motor for mitochondrial movement in vertebrate cells.

Myo19 encodes a novel metazoan myosin

Previous sequence analysis predicted an uncharacterized myosin gene on human chromosome 17q12 that appeared to represent a novel myosin class [7,8]. Using the database sequence FLJ22865 (*myohd1*, GI:14286205), we generated PCR primers to clone the full-length coding region of this putative myosin from human pancreas cDNA. Sequence analysis of the PCR-amplified clone revealed a 970aa coding region consisting of a myosin motor domain, a neck

Corresponding author: Omar A. Quintero, Phone: (717) 531-8997, FAX: (717) 531-7667, oaq100@psu.edu.

region containing three IQ motifs, and a short tail (Figure 1A). The Myo19 motor domain shares ~35% sequence identity with the motor domains of human skeletal muscle myosin, Myo5a, and Myo6. The motor contains the conserved GESGAGKT sequence from the P-loop, DXXGFE sequence from switch-2 (DVYGFE), and a slightly divergent MEAFGNACTLRNNNSSRFGK in the switch-1 region (Supplemental Figure 1A, reviewed in [9]). Myo19 has a glutamine at the TEDS position, indicating that it is not regulated by heavy-chain phosphorylation at this site [10]. The three IQ motifs in the neck region are expected to bind calmodulin or calmodulin-like light chains [11]. The 146aa tail domain is basic (pI ~9.2), and is not predicted to form a coiled-coil [12]. Interestingly, the tail has no obvious sequence homology with other proteins in the databases, except for other Myo19 orthologs (Supplemental Figure 1B). FLJ22865 corresponds to a 770aa Myo19 sequence lacking 4 sequential exons from the core motor domain and is thus likely to represent either an aberrant cDNA or a splice form with a non-functional motor. Clear orthologs of human Myo19 are present in multiple vertebrate species including mouse (GI:56206893), chicken (GI:118100337), *Xenopus laevis* (GI:62185680), and zebrafish (GI:189519181). At the amino acid level, human Myo19 (970aa) exhibits 82% identity to mouse Myo19 (963aa) and 56% identity to *Xenopus laevis* Myo19 (971aa). Although Myo19 arose early in metazoan evolution, it appears to have been lost from lineages leading to *Drosophila* and *C. elegans* [8].

Myo19 is expressed in multiple tissues and cell lines

To determine the tissue expression pattern of Myo19, we probed a Northern blot using a sequence from the 3′ non-coding region. A band of approximately 4.2kb was detected in multiple tissues (Figure 1B). Analysis of EST databases (Supplemental Table 1) and the Allen Brain Atlas (http://www.brain-map.org) indicate that Myo19 is broadly expressed in vertebrate cells, tissues, and tumors. Antibodies raised against the Myo19 peptide AKELDGVEEKHFS (aa 829-841) detected a protein of the expected size of ~109kD in western blots of human and other primate cell lines (Figure 1C). We also detected Myo19 in mouse cell lines (B16-F1 and CAD), but the signal was weaker, likely due to sequence differences in the antibody target (**S**KELDG**M**EEK**PMP** in mouse).

Myo19 localizes to mitochondria

To determine the cellular localization of Myo19, we immunostained multiple cell lines (A549, HeLa, and COS-7) with anti-Myo19 antibody. Colocalization with Mitotracker-stained mitochondria revealed clear and striking localization of endogenous Myo19 to mitochondria (Figure 2A, Supplemental Figure 2A). To determine the region of Myo19 required for mitochondrial localization, we generated a series of GFP-constructs containing different regions of the Myo19 protein. Full-length GFP-Myo19 and a “tail” construct containing amino acids 801-970 both clearly localized to mitochondria (Figure 2B, Supplemental Figure 2B). However, a construct containing the motor domain and IQ motifs (amino acids 1-828) did not localize to mitochondria and exhibited diffuse cytoplasmic staining with some brighter puncta (Figure 2B, Supplemental Figure 2B). To test if Myo19 is anchored to the mitochondrial outer membrane via insertion of a c-terminal transmembrane helix [13], we added GFP to the c-terminus [14]. Expression of either a Myo19 tail or a full-length Myo19 construct GFP-tagged at the c-terminus resulted in mitochondrial localization. Taken together, these data indicate that the tail domain of Myo19 is necessary and sufficient for mitochondrial localization via a mechanism that is unlikely to involve a c-terminal transmembrane helix (Figure 2C).

To test whether Myo19 is stably associated with mitochondria, we used fluorescence recovery after photobleaching (FRAP) analysis (Movie S01). GFP-Myo19 tail displayed recovery dynamics similar to those of cytochrome b_5 (GFP-Cytob5-RR), a transmembrane protein that localizes to the outer mitochondrial membrane [15] (Supplemental Figure 3). Six minutes

following the bleaching event, neither construct recovered its fluorescence completely (52±7% recovery GFP-Myo19 tail, n=16, 53±4% GFP-cytob5-RR, n=10), and both constructs had a time to 50% maximum recovery ($t_{1/2}$) of greater than two minutes (Supplemental Figure 3B). The lack of fluorescence recovery cannot be accounted for by simple photo-fading due to visualization of the samples, as unbleached regions of the same or neighboring cells did not lose significant amounts of fluorescence over the same time period. While the Myo19 tail shares no obvious sequence homology with class I myosin tails, both Myo19 and class I myosin tail regions contain a large number of basic residues. In class I myosins, these basic residues mediate the binding to specific phospholipids in the membrane [16]. Although it is possible that binding to acidic phospholipids may anchor Myo19 to mitochondria, it is unlikely that the Myo19 and Myo1 mechanisms are identical, as the FRAP dynamics of Myo1A are much faster (~80% recovery in less than 1 minute) than that of Myo19 [17]. These data indicate that Myo19 does not rapidly exchange and suggests that it is tightly associated with the mitochondrial outer membrane.

Expressing GFP-Myo19 alters mitochondrial dynamics

To test if Myo19 functions in actin-based mitochondrial motility, we transfected A549 cells with GFP-Myo19, pDsRed2-Mito (as a control) or both plasmids in combination and then used time-lapse imaging to assess mitochondrial dynamics. In control A549 cells, the vast majority of mitochondria remained largely in place with only small “jostling” movements (Movie S02). Expressing GFP-Myo19, however, led to a dramatic increase in mitochondrial motility (Movie S03, Figure 3A). In approximately 40% of the cells expressing GFP-Myo19, the majority of mitochondria moved continuously for many microns with one end of the mitochondrion leading. The leading end was often wider than the trailing end, resulting in a tadpole-like appearance (Figure 3B, Movie S03). Unlike microtubule-dependent movements, these mitochondria did not follow linear tracks and their movements were not obviously directed to or from the cell center (Figure 3A, Movie S04).

To quantify the increase in mitochondrial motility induced by GFP-Myo19, we determined a “Displacement Index” (D.I.) by dividing the area over which mitochondrial network moved in a 3:20 (min:sec) time-lapse by the area occupied by mitochondria in the first frame of the recording (Supplemental Figure 4). If the mitochondrial network remained perfectly stationary, then D.I.=1. Control A549 cells had a D.I. of 1.2±0.1 (n=10 cells) while the D.I. in GFP-Myo19 cells increased by 75% to 2.1±0.7 (n=28 cells, $p<0.0003$, Supplemental Figure 4D). Additionally, the values for D.I. from cells expressing GFP-Myo19 alone were not statistically different from the D.I. values calculated from cells expressing both pDsRed2-Mito and GFP-Myo19 (2.2±0.16, n=19 cells). These data demonstrate that expression of GFP-Myo19 dramatically increases mitochondrial dynamics.

As an additional measure of mitochondrial motility, we also we calculated the average velocities of randomly selected mitochondria in control A549 cells and A549 cells transfected with GFP-Myo19. The velocities of control mitochondria formed a broad peak centered at relatively low velocities, while the velocity distribution for GFP-Myo19 mitochondria was shifted to the right and had an additional small peak in the 50-75 nm/s range (Figure 3C). The average velocity of randomly selected mitochondria in the control cells was 16±1nm/s (n=121 mitochondria, 12 cells). Expressing GFP-Myo19 resulted in an average velocity of 29±2nm/s (n=153 mitochondria, 8 cells; $p<0.0001$), a 75% increase over control cells. Expression of GFP-Myo19 in conjunction with pDsRed2-Mito also resulted in a similar increase in velocity over control cells (31±2nm/s, n= 62 mitochondria, 8 cells; $p<0.0001$), and was not significantly different from cells expressing GFP-Myo19 alone. Since these measurements included mitochondria from all GFP-Myo19 cells, including those that exhibited little movement, the average velocity in the ~40% of A549 cells that exhibited increased mitochondrial movement

would be even greater. When velocities were measured by selecting for mitochondria that were exhibiting long-range, end-on movements, the mitochondria in GFP-Myo19 cells that were moving continuously had an average velocity of 73±3nm/s (n=125 mitochondria, 8 cells). In control cells the average of moving mitochondria was 102±7nm/s (n=27 mitochondria, 6 cells). These values are similar to the value of the additional minor peak in the histograms of velocities for randomly chosen mitochondria.

GFP-Myo19 induced mitochondrial motility is actin-dependent and requires the Myo19 motor domain

We hypothesize that the movements of mitochondria we observed are powered by interactions between the Myo19 motor domain and randomly organized actin filaments. To test if the observed gain of function requires the Myo19 motor domain, we measured the D.I. (Supplemental Figure 4C) and average velocity of mitochondria in A549 cells expressing GFP-Myo19 tail. Neither the D.I. (1.5±0.1, n=17 cells) nor the velocity of randomly chosen mitochondria (20±3 nm/s, n=38 mitochondria, 4 cells) were significantly different from those measures in control cells. Similar results were also obtained in cells coexpressing GFP-Myo19 tail and pDsRed2-Mito (D.I.=1.5±0.1, n=19 cells; 21±2nm/s, n=55 mitochondria, 8 cells). In either case, expression of GFP-Myo19 tail did not increase mitochondrial motility, indicating that the motor domain of Myo19 is required for enhanced mitochondrial dynamics.

To test if these movements are indeed actin-based, cells expressing full-length GFP-Myo19 were treated with 15μM nocodazole to disrupt microtubules or 500nM latrunculin B to disrupt F-actin. This dose of nocodazole was sufficient to disrupt the distribution of the endoplasmic reticulum within 5 minutes (data not shown).

Mitochondrial movements induced by GFP-Myo19 were insensitive to nocodazole treatments (Figure 4A, Movies S05, S06, and S07). These mitochondria continued to display movement over many microns and the tadpole shape remained. However, upon addition of latrunculin B to nocodazole-treated cells, the end-on, directed movements ceased (Figure 4B, Movies S05, S06, and S07). In addition, the mitochondria lost their asymmetric shape within 2 minutes of latrunculin B treatment (Figure 4C). Treatment of cells with latrunculin B without nocodazole pretreatment also resulted in a prompt cessation of end-on mitochondrial movement and a rapid loss of the asymmetric shape, demonstrating that both the motility and altered shape are dependent on the presence of F-actin (Movie S09).

An alternative to the hypothesis that the motor activity of Myo19 powers mitochondria movements would be that Myo19 recruits F-actin to the mitochondria and actin polymerization pushes the organelle via a mechanism similar to *Listeria* motility [18-20]. However, mitochondria in GFP-Myo19-expressing cells did not exhibit phase-dense tails similar to those reported for *Listeria* (Figure 3B,Movie S04 and S06). To determine if GFP-Myo19-labeled mitochondria lack actin tails, we co-expressed the non-perturbing F-actin label, mRFP-utrophin [21] in combination with full-length GFP-Myo19. Although we observed mRFP-utrophin labeling of other F-actin structures such as filopodia, we did not observe F-actin tails behind GFP-Myo19 labeled mitochondria (Supplemental Figure 5A, Movies 11 and S12). Additionally, we took time-lapse movies of GFP-Myo19 expressing cells on gridded coverslips, allowing us to locate cells with increased mitochondrial dynamics prior to fixation and phalloidin staining. Again, the mitochondria lacked *Listeria*-like actin tails (Supplemental Figure 5B, Movie S13).

When GFP-utrophin-expressing A549 cells were infected with fluorescent *Listeria*, actin clouds and actin tails associated with the bacteria (Supplemental Figure 5C, Movie S14). Taken

together these data indicate that Myo19-induced movement is unlikely to be due to polymerization-mediated pushing.

Although the lack of directed mitochondrial movement in control A549 cells was ideal for gain-of-function experiments, it was problematic for loss-of-function studies. Since expression of myosin tails has been widely used as a dominant negative approach to investigate the functions of unconventional myosins [22-24] and previous work has shown that mitochondrial motility in neurites is partially actin-based [25-27], we expressed the Myo19 tail in CAD cells [28] to test the function of Myo19 in normal mitochondrial dynamics. In CAD cell neurites, where mean run lengths can be measured relatively easily, expressing GFP-Myo19 tail resulted in a 40% decrease in mitochondrial run length from 1.4±0.3μm (n=141) for control cell (pDsRed2-Mito labeled) mitochondria to 0.8±0.1μm (n=250) for GFP-Myo19 tail-labeled mitochondria (Figure 4D, $p<0.03$). This suggests that Myo19 function is indeed necessary for normal mitochondrial dynamics.

Myo19 is a novel mitochondrial associated myosin that is likely to function in actin-based mitochondrial dynamics

Taken together, our data strongly suggest that Myo19 is a broadly expressed mitochondrial myosin involved in actin-mediated mitochondrial movements and positioning. Endogenous Myo19 localizes to mitochondria, and the FRAP and truncation analyses indicate that Myo19 localizes to mitochondria via its tail domain. Expression of full-length GFP-Myo19 protein induces a dramatic increase in mitochondrial motility in A549 cells, and we observed similar increases in mitochondrial motility in COS-7 and B16-F1 cells (data not shown). As predicted for myosin-driven movements, these movements require the motor domain, as GFP-Myo19 tail expression did not result in the enhancement of mitochondrial dynamics observed in cells expressing full length GFP-Myo19. Additionally, these movements are indeed actin based, as GFP-Myo19 induced movements cease upon destabilization of the actin network. Since the striking increase in mitochondrial motility was not observed in 100% of the cells expressing GFP-Myo19, it is likely that additional factors regulate Myo19 function and/or mitochondrial movement. Whether those conditions are related to the amount of Myo19 on the mitochondrial surface or activation state of Myo19 motor has yet to be determined. Expression of the GFP-Myo19 tail may impact activity level of Myo19 on the mitochondrial surface by displacing endogenous, functional Myo19. In CAD cell neurites, expression of GFP-Myo19 tail resulted in a 40% decrease in mitochondrial run lengths, lending further support to the hypothesis that Myo19 is involved in mitochondrial dynamics.

The localization and dynamics of mitochondria are critical to their function and disruption of these processes leads to human disease [29,30]. Mitochondrial localization and dynamics have been shown to involve both microtubules and actin [31-35]. However, the mechanism of actin-based mitochondrial movements in vertebrates remains unclear [36]. Our discovery of a novel class of myosin that localizes to mitochondria provides a possible molecular mechanism for actin-based mitochondrial movements.

Supplementary Material

Refer to Web version on PubMed Central for supplementary material.

Acknowledgments

This work was supported by a SPIRE postdoctoral training grant NIH/GM00678 to OAQ, and NIH/NIDCD DC03299 to REC. It was also supported in part by a Summer Fellowship (The Laura and Arthur Colwin Endowed Summer Research Fellowship Fund and The E. E. Just Endowed Research Fellowship Fund) at the Marine Biological Laboratory (Woods Hole, MA) to OAQ and by a Linkage Fellowship from the American Society for Cell Biology to

OAQ. We would like to thank William Bement for providing the mRFP-utrophin and GFP-utrophin plasmids, Nica Borgese for the GFP-Cytob5-RR plasmid, Donna Chikaraishi for providing CAD cells, Jo Rae Wright for providing A549 cells, Lynne Cassimeris for assistance with confocal microscopy, and Dale Callaham for assistance with confocal microscopy (NSF/BBS 8714235). We would also like to thank Ryan Mehl, Peter Fields, and Christopher Yengo for access to equipment and supplies, and Michael Kerber for assistance with tracking mitochondria and critical reading of this manuscript. We are particularly grateful to Julie Theriot for her generosity and assistance with imaging *Listeria*-infected cells, and to Peter Lauer for providing the tagRFP-*Listeria*.

References

1. Collins TJ, Berridge MJ, Lipp P, Bootman MD. Mitochondria are morphologically and functionally heterogeneous within cells. EMBO J 2002;21:1616–1627. [PubMed: 11927546]
2. Rube DA, van der Bliek AM. Mitochondrial morphology is dynamic and varied. Mol Cell Biochem 2004:256–257. 331–339.
3. Wallace DC. Mitochondrial diseases in man and mouse. Science 1999;283:1482–1488. [PubMed: 10066162]
4. Chen H, Chomyn A, Chan DC. Disruption of fusion results in mitochondrial heterogeneity and dysfunction. J Biol Chem 2005;280:26185–26192. [PubMed: 15899901]
5. Chan DC. Mitochondria: dynamic organelles in disease, aging, and development. Cell 2006;125:1241–1252. [PubMed: 16814712]
6. Sokac AM, Bement WM. Regulation and expression of metazoan unconventional myosins. Int Rev Cytol 2000;200:197–304. [PubMed: 10965469]
7. Berg JS, Powell BC, Cheney RE. A millennial myosin census. Mol Biol Cell 2001;12:780–794. [PubMed: 11294886]
8. Odronitz F, Kollmar M. Drawing the tree of eukaryotic life based on the analysis of 2,269 manually annotated myosins from 328 species. Genome Biol 2007;8:R196. [PubMed: 17877792]
9. Cope MJ, Whisstock J, Rayment I, Kendrick-Jones J. Conservation within the myosin motor domain: implications for structure and function. Structure 1996;4:969–987. [PubMed: 8805581]
10. Bement WM, Mooseker MS. TEDS rule: a molecular rationale for differential regulation of myosins by phosphorylation of the heavy chain head. Cell Motil Cytoskeleton 1995;31:87–92. [PubMed: 7553910]
11. Cheney RE, Mooseker MS. Unconventional myosins. Curr Opin Cell Biol 1992;4:27–35. [PubMed: 1558751]
12. Lupas A, Van Dyke M, Stock J. Predicting coiled coils from protein sequences. Science 1991;252:1162–1164.
13. Borgese N, Colombo S, Pedrazzini E. The tale of tail-anchored proteins: coming from the cytosol and looking for a membrane. J Cell Biol 2003;161:1013–1019. [PubMed: 12821639]
14. Horie C, Suzuki H, Sakaguchi M, Mihara K. Characterization of signal that directs C-tail-anchored proteins to mammalian mitochondrial outer membrane. Mol Biol Cell 2002;13:1615–1625. [PubMed: 12006657]
15. Borgese N, Gazzoni I, Barberi M, Colombo S, Pedrazzini E. Targeting of a tail-anchored protein to endoplasmic reticulum and mitochondrial outer membrane by independent but competing pathways. Molecular Biology of the Cell 2001;12:2482–2496. [PubMed: 11514630]
16. Hokanson DE, Ostap EM. Myo1c binds tightly and specifically to phosphatidylinositol 4,5-bisphosphate and inositol 1,4,5-trisphosphate. Proc Natl Acad Sci U S A 2006;103:3118–3123. [PubMed: 16492791]
17. Tyska MJ, Mooseker MS. MYO1A (brush border myosin I) dynamics in the brush border of LLC-PK1-CL4 cells. Biophys J 2002;82:1869–1883. [PubMed: 11916846]
18. Mogilner A, Oster G. Force generation by actin polymerization II: the elastic ratchet and tethered filaments. Biophys J 2003;84:1591–1605. [PubMed: 12609863]
19. Tilney LG, Portnoy DA. Actin filaments and the growth, movement, and spread of the intracellular bacterial parasite, Listeria monocytogenes. J Cell Biol 1989;109:1597–1608. [PubMed: 2507553]
20. Theriot JA, Mitchison TJ, Tilney LG, Portnoy DA. The rate of actin-based motility of intracellular Listeria monocytogenes equals the rate of actin polymerization. Nature 1992;357:257–260. [PubMed: 1589024]

21. Burkel BM, von Dassow G, Bement WM. Versatile fluorescent probes for actin filaments based on the actin-binding domain of utrophin. Cell Motil Cytoskeleton 2007;64:822–832. [PubMed: 17685442]
22. Reck-Peterson SL, Novick PJ, Mooseker MS. The tail of a yeast class V myosin, myo2p, functions as a localization domain. Mol Biol Cell 1999;10:1001–1017. [PubMed: 10198053]
23. Wu X, Wang F, Rao K, Sellers JR, Hammer JA 3rd. Rab27a is an essential component of melanosome receptor for myosin Va. Mol Biol Cell 2002;13:1735–1749. [PubMed: 12006666]
24. Roland JT, Kenworthy AK, Peranen J, Caplan S, Goldenring JR. Myosin Vb interacts with Rab8a on a tubular network containing EHD1 and EHD3. Mol Biol Cell 2007;18:2828–2837. [PubMed: 17507647]
25. Morris RL, Hollenbeck PJ. Axonal transport of mitochondria along microtubules and F-actin in living vertebrate neurons. J Cell Biol 1995;131:1315–1326. [PubMed: 8522592]
26. Hollenbeck PJ. The pattern and mechanism of mitochondrial transport in axons. Front Biosci 1996;1:d91–102. [PubMed: 9159217]
27. Ligon LA, Steward O. Role of microtubules and actin filaments in the movement of mitochondria in the axons and dendrites of cultured hippocampal neurons. J Comp Neurol 2000;427:351–361. [PubMed: 11054698]
28. Qi Y, Wang JK, McMillian M, Chikaraishi DM. Characterization of a CNS cell line, CAD, in which morphological differentiation is initiated by serum deprivation. J Neurosci 1997;17:1217–1225. [PubMed: 9006967]
29. Zuchner S, Mersiyanova IV, Muglia M, Bissar-Tadmouri N, Rochelle J, Dadali EL, Zappia M, Nelis E, Patitucci A, Senderek J, et al. Mutations in the mitochondrial GTPase mitofusin 2 cause Charcot-Marie-Tooth neuropathy type 2A. Nat Genet 2004;36:449–451. [PubMed: 15064763]
30. Delettre C, Lenaers G, Pelloquin L, Belenguer P, Hamel CP. OPA1 (Kjer type) dominant optic atrophy: a novel mitochondrial disease. Mol Genet Metab 2002;75:97–107. [PubMed: 11855928]
31. Boldogh IR, Yang HC, Nowakowski WD, Karmon SL, Hays LG, Yates JR 3rd, Pon LA. Arp2/3 complex and actin dynamics are required for actin-based mitochondrial motility in yeast. Proc Natl Acad Sci U S A 2001;98:3162–3167. [PubMed: 11248049]
32. Altmann K, Frank M, Neumann D, Jakobs S, Westermann B. The class V myosin motor protein, Myo2, plays a major role in mitochondrial motility in Saccharomyces cerevisiae. J Cell Biol 2008;181:119–130. [PubMed: 18391073]
33. Minin AA, Kulik AV, Gyoeva FK, Li Y, Goshima G, Gelfand VI. Regulation of mitochondria distribution by RhoA and formins. J Cell Sci 2006;119:659–670. [PubMed: 16434478]
34. Nangaku M, Sato-Yoshitake R, Okada Y, Noda Y, Takemura R, Yamazaki H, Hirokawa N. KIF1B, a novel microtubule plus end-directed monomeric motor protein for transport of mitochondria. Cell 1994;79:1209–1220. [PubMed: 7528108]
35. Tanaka Y, Kanai Y, Okada Y, Nonaka S, Takeda S, Harada A, Hirokawa N. Targeted disruption of mouse conventional kinesin heavy chain, kif5B, results in abnormal perinuclear clustering of mitochondria. Cell 1998;93:1147–1158. [PubMed: 9657148]
36. Hollenbeck PJ, Saxton WM. The axonal transport of mitochondria. J Cell Sci 2005;118:5411–5419. [PubMed: 16306220]

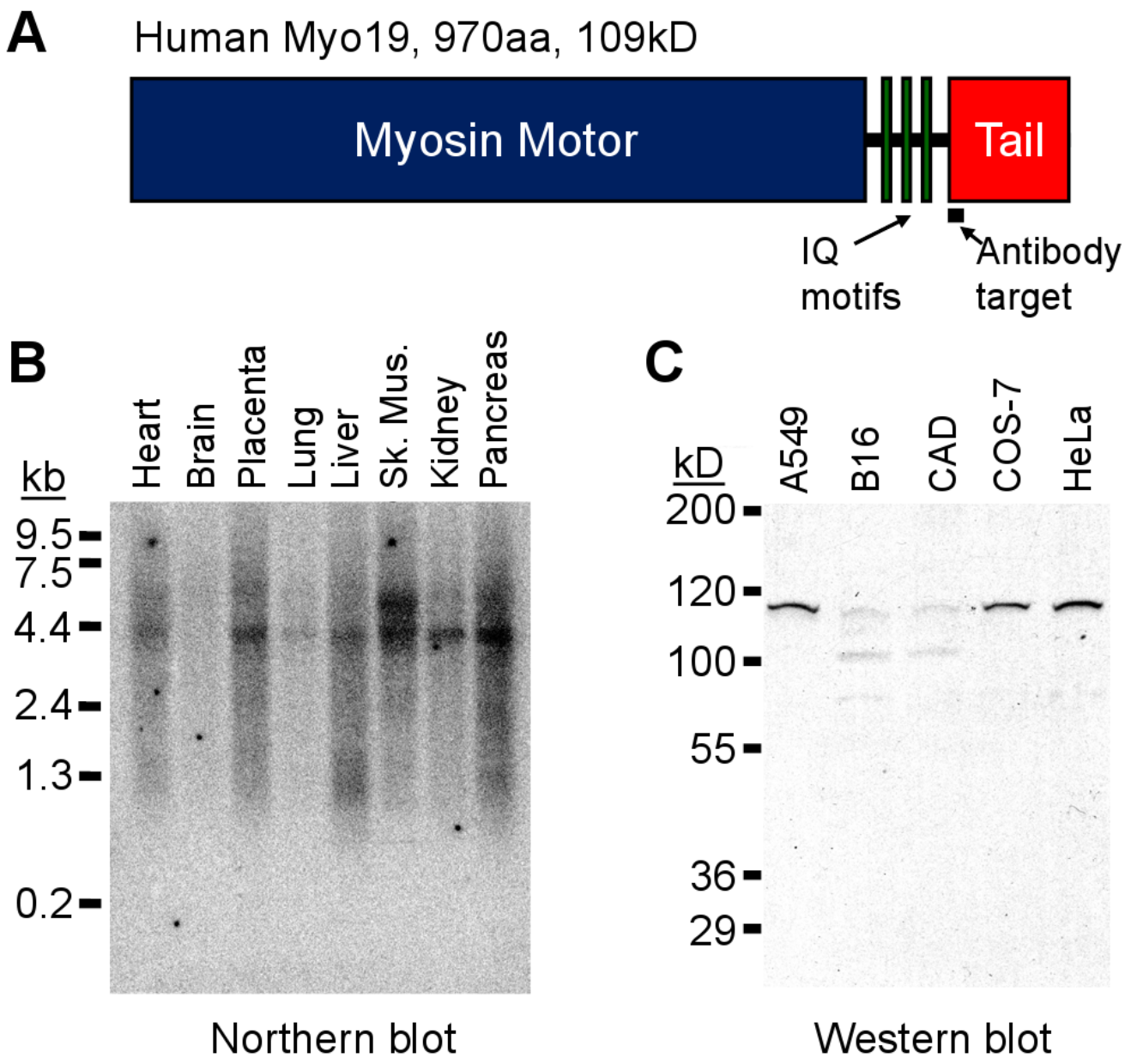

Figure 1.

Myo19 is expressed in multiple tissues and cell lines. (A) Human Myo19 is predicted to consist of a motor domain, neck region with three IQ motifs, and a short tail domain. (B) A 4.2kb messenger RNA encoding for the Myo19 protein was detected by Northern blot analysis in multiple human tissues at varying levels. In skeletal muscle, a larger mRNA also appeared to react with the probe. Although the brain sample in this blot did not show strong reactivity, EST databases indicate that Myo19 is expressed in brain. Ladder indicates sizes of molecular weight markers in kb. (C) A protein of approximately 109kD was detected by western blot using antibodies raised against a peptide from the tail of human Myo19. This antibody cross-reacted poorly with rodent cell lines (B16F1 and CAD), but was able to detect Myo19 in human (HeLa

and A549) and monkey cell lines (COS-7). Ladder indicates sizes of molecular weight markers in kD.

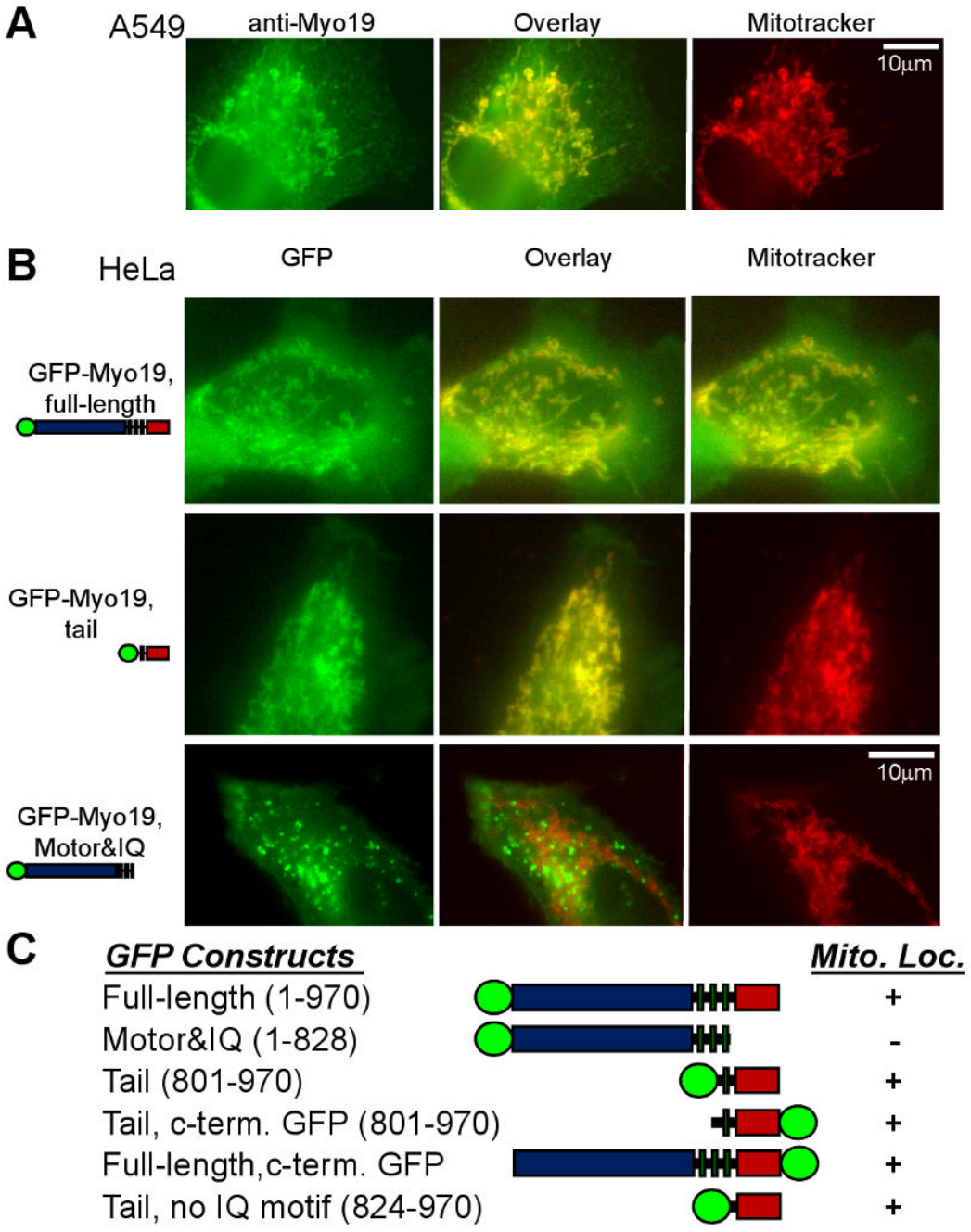

Figure 2.

Myo19 localizes to mitochondria. (A) Antibodies raised against a peptide from human Myo19 (green) strongly label Mitotracker-stained mitochondria (red) in A549 cells (shown), HeLa cells, and COS-7 cells. (B) Both full length GFP-Myo19 and a tail construct (green) also colocalize with Mitotracker-labeled mitochondria (red), in HeLa cells (shown), A549 cells, and COS-7 cells. Constructs consisting of the motor domain and IQ motifs do not localize to mitochondria. (C) Amino acids 824-970 are necessary and sufficient for mitochondrial localization as GFP constructs consisting of only this sequence of amino acids localize to mitochondria. GFP is represented by a green oval in the domain diagrams of the constructs in panels (B) and (C). Scale bars in (A) and (B) equal 10 μm.

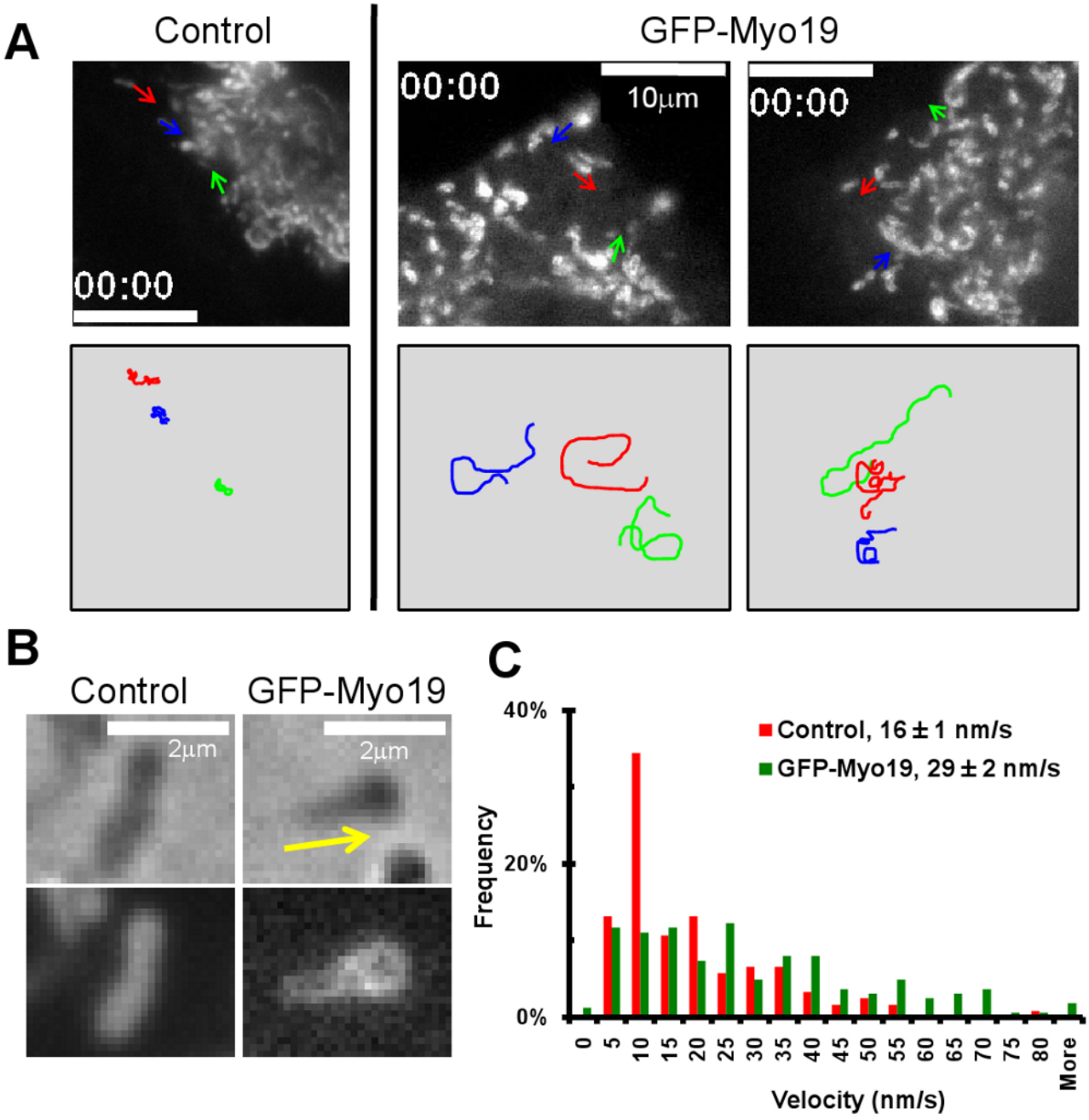

Figure 3.

Expressing GFP-Myo19 increases mitochondrial motility. (A) Mitochondria in control A549 cells expressing pDsRed2-Mito showed little movement. Expression of GFP-Myo19 greatly increases mitochondrial movements, and the lengths of those movements. These movements were often non-linear, and did not necessarily correspond to movements towards or away from the nucleus. Arrows in the top panels represent the initial direction of movement for the indicated mitochondria, and paths taken by those mitochondria (over 4 minutes) are represented in the bottom panel. (B) In addition to inducing motility of mitochondria in A549 cells, expression of full-length GFP-Myo19 often led to mitochondria with an obvious taper, where the trailing end was narrower than the leading end, as can be seen by phase contrast imaging

or fluorescence imaging. Tapered mitochondria were only occasionally observed in cells not expressing GFP-Myo19. Arrow indicates the direction of movement. (C) A histogram of velocities of randomly selected mitochondria shows that expression of full length GFP-Myo19 led to a 75% increase in the average mitochondrial velocity (*$p<0.0003$). For pDsRed2-Mito (control) cells, n=121 mitochondria (12 cells). For GFP-Myo19 cells, n=153 mitochondria (8 cells). Velocities in legend are mean±SEM. Images in (A) are from Movie S02 for the control cell, and Movie S03 for the GFP-Myo19-expressing cell.

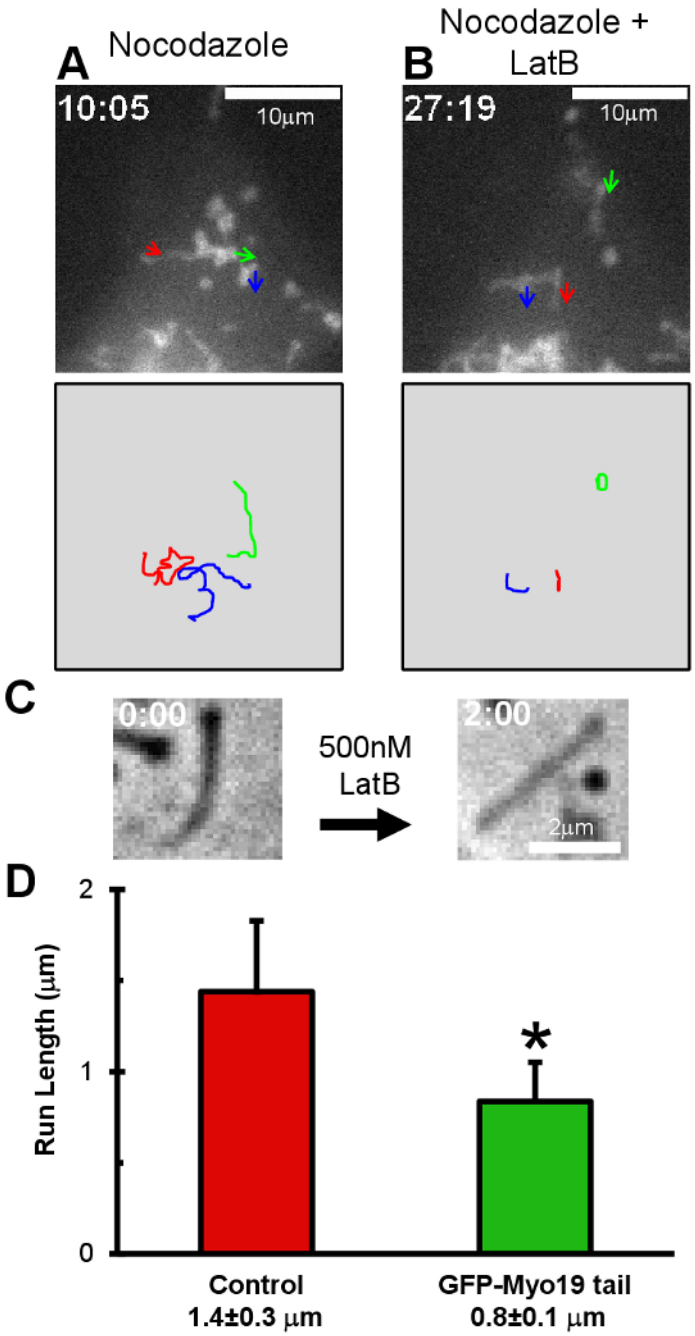

Figure 4.

GFP-Myo19 induced movements in A549 cells are actin-dependent, and expression of GFP-Myo19 tail decreases mitochondrial run lengths in CAD cells. (A) As can be seen in Supplemental Movie S05, microtubule disruption with 15µM nocodazole failed to inhibit mitochondrial movements or shape change in GFP-Myo19 expressing A549 cells (drug added at 1minute, 40 seconds). Arrows in the top panels represent the initial direction of movement, and the corresponding tracks over the next four minutes are shown in the bottom panels. (B) Disruption of actin with the addition of 500nM latrunculin B halted mitochondrial movements (drug added at 26:19). (C) Latrunculin B also disrupted the tapered mitochondrial shape within two minutes of addition, as visualized by phase contrast microscopy. (D) Expression of GFP-

Myo19 tail in differentiated CAD cells resulted in a 40% decrease in mitochondrial run length in neurites, as compared to control cells (*$p<0.03$, n=141 for pDsRed2-Mito control, n=250 for GFP-Myo19 tail). The average velocity of moving mitochondria were similar in control cells (75±11nm/s, n=16) and in cells expressing GFP-Myo19 tail (65±5nm/s, n=69). Images in (A) and (B) correspond to portions of Movie S05. Timestamp represents min:sec.